

Chapter 8

Flux-Based O₃ Risk Assessment for Japanese Temperate Forests

Mitsutoshi Kitao, Yukio Yasuda, Masabumi Komatsu, Satoshi Kitaoka, Kenichi Yazaki, Hiroyuki Tobita, Kenich Yoshimura, Takafumi Miyama, Yuji Kominami, Yasuko Mizoguchi, Katsumi Yamanoi, Takayoshi Koike, and Takeshi Izuta

Abstract Ground-level ozone (O₃) levels are expected to increase over the twenty-first century, particularly in the region of East Asia. We performed an O₃ flux-based risk assessment of C sequestering capacity in an old cool temperate deciduous forest, consisting of O₃-sensitive Japanese beech (*Fagus crenata*), and in a warm temperate deciduous and evergreen forest dominated by O₃-tolerant Konara oak (*Quercus serrata*), based on long-term CO₂ flux observations. Light-saturated

M. Kitao (✉) • M. Komatsu • S. Kitaoka • K. Yazaki • H. Tobita
Department of Plant Ecology, Forestry and Forest Products Research Institute,
Matsunosato 1, Tsukuba 305-8687, Japan
e-mail: kitao@ffpri.affrc.go.jp; kopine@ffpri.affrc.go.jp; skitaoka3104@gmail.com;
kyazaki@ffpri.affrc.go.jp; tobi@ffpri.affrc.go.jp

Y. Yasuda
Tohoku Research Center, Forestry and Forest Products Research Institute,
Nabeyashiki 92-25, Morioka 020-0123, Japan
e-mail: yassan@ffpri.affrc.go.jp

K. Yoshimura • T. Miyama • Y. Kominami
Kansai Research Center, Forestry and Forest Products Research Institute,
Nagaikyutaroh 68, Kyoto 612-0855, Japan
e-mail: mt_everysashi@hotmail.com; tmiyama@affrc.go.jp; kominy@ffpri.affrc.go.jp

Y. Mizoguchi • K. Yamanoi
Hokkaido Research Center, Forestry and Forest Products Research Institute,
Hitsujigaoka 7, Sapporo 062-8516, Japan
e-mail: pop128@affrc.go.jp; yamanoi@ffpri.affrc.go.jp

T. Koike
Department of Forest Science, Hokkaido University, Sapporo 060-8589, Japan
e-mail: tkoike@for.agr.hokudai.ac.jp

T. Izuta
Institute of Agriculture, Tokyo University of Agriculture and Technology,
Fuchu, Tokyo 183-8509, Japan
e-mail: izuta@cc.tuat.ac.jp

gross primary production, as a measure of C sequestering capacity, declined earlier in the late-growth season with increasing cumulative O₃ uptake, suggesting an earlier autumn senescence in the O₃-sensitive beech forest, but not in the O₃-tolerant oak forest.

Keywords C sequestration • O₃ flux • O₃-sensitive forest • O₃-tolerant forest • Deciduous temperate forests

8.1 Introduction

In Japan, which is located on the edge of East Asia, a continuous increase in O₃ concentration has been observed since the latter half of the 1980s, partly due to pollutants advected from foreign sources, particularly in East Asia (Richter et al. 2005; Ohara et al. 2008; Nagashima et al. 2003; Akimoto 2003). Since 2000, the flux tower sites of the Forestry and Forest Products Research Institute (FFPRI) have monitored CO₂, energy, and water vapor fluxes in several Japanese forests with different tree species. Although O₃ is known to be a detrimental air pollutant for trees, as it reduces the photosynthetic rate, increases the respiration rate, and accelerates leaf senescence (Matyssek et al. 2010), few studies have been conducted to assess the O₃ risk in forests directly. Thus, we have a unique chance to assess the O₃ risk in Japanese forests based on the long-term CO₂ flux observations.

O₃ flux-based risk assessment is more essential than O₃ exposure-based risk assessment for evaluating the physiological effects of O₃ on plants (Emberson et al. 2000; Matyssek et al. 2007). To estimate O₃ fluxes at the forest level, canopy-level stomatal conductance is required, as well as O₃ concentration over the forest, which is generally estimated by the Penman–Monteith (P–M) equation, based on energy and water flux over a forest (Gerosa et al. 2005; Monteith 1981). However, the use of this approach is valid only when the entire evaporation process in the canopy takes place through stomatal transpiration. In this context, it is difficult to conduct a continuous estimation of the canopy-level stomatal conductance using the P–M approach in temperate deciduous forests, which have regular rainfall and a period when the canopy is not closed, in spring and autumn (Biftu and Gan 2000).

To solve this problem, we have developed a novel approach (Kitao et al. 2014) combining the P–M approach with a semi-empirical photosynthesis-dependent stomatal model (Ball–Woodrow–Berry [BWB] model; Ball et al. 1987), where photosynthesis, relative humidity, and CO₂ concentration are assumed to regulate stomatal conductance. Based on the BWB model, leaf-level stomatal conductance (g_s) is estimated as:

$$g_s = g_{\min} + a A_g \text{rh} / C_s \quad (8.1)$$

where g_{\min} denotes the minimum conductance in the dark, a is an empirical scaling parameter, A_g the gross photosynthetic rate, rh the relative humidity, and C_s the leaf surface CO₂ concentration.

In the present study, we applied the modified BWB model to estimate canopy-level stomatal conductance (G_s) taking into account the non-linear response of canopy stomatal conductance to relative humidity (Fares et al. 2013) as:

$$G_s = G_{\min} + ab^{\text{th}} \text{GPP} / C_s \quad (8.2)$$

where G_{\min} denotes the canopy-level minimum conductance in the dark, a and b are empirical scaling parameters, and GPP is the gross primary production (= net ecosystem exchange [NEE] – respiration of ecosystem [R_{eco}]). We first determined the coefficients in the equation, using G_s derived by the (P–M) equation when the canopy was closed from June to August for the beech forest, and G_s derived by the (P–M) equation from June to September for the oak forest without rain (>1 mm within 24 h) for each year. Then we estimated the stomatal conductance over the canopy of temperate deciduous forests continuously, using this novel approach combining the P–M approach with a photosynthesis-dependent stomatal model (Kitao et al. 2014).

Based on the above approach, we performed flux-based assessments of O₃ effects on photosynthetic CO₂ uptake in a cool temperate deciduous forest, consisting of O₃-sensitive deciduous broadleaf tree species, Japanese beech (*Fagus crenata* Blume; 70–80 years old), and a warm temperate mixed deciduous and evergreen broadleaf forest, dominated by O₃-tolerant deciduous broadleaf tree species, Konara oak (*Quercus serrata* Thunb. ex. Murray; approximately 30 years old) (Yasuda et al. 2012; Kominami et al. 2012; Yamaguchi et al. 2011; Kitao et al. 2015).

8.2 Study Sites

The Appi forest meteorology research site (40° 00' N, 140° 56' E, 825 m above sea level) is located on the Appi highland in Iwate Prefecture, Japan (details of which are described in Yasuda et al. 2012) (Fig. 8.1). The site is located in a secondary cool temperate deciduous broadleaf forest primarily consisting of the Japanese beech (*Fagus crenata* Blume), which was approximately 80 years old. The canopy height was measured to be 19–20 m in 2009. There is not much vegetation on the forest floor, and evergreen trees are rarely observed. It snows heavily from November to May, with the snow depth reaching 2 m. The annual mean temperature was 5.9 °C (in 2000–2006), annual precipitation was 1,869 mm (in 2007–2009), and annual mean solar radiation was 12.7 MJ m⁻² day⁻¹ (in 2000–2006). The soil was classified as moderately moist brown forest soil.

The Yamashiro forest hydrology research site (34° 47' N, 135° 50' E, 220 m above sea level) is situated in the southern part of Kyoto Prefecture, Japan (details of which are described in Kominami et al. 2012) (Fig. 8.2). The site is located in a warm temperate mixed deciduous and evergreen broadleaf forest, which is built upon weathered granite. After an invasion by pine wilt disease in the 1980s, Konara oak (*Quercus serrata* Thunb. ex. Murray) has taken over and the forest is now

Fig. 8.1 Cool temperate deciduous forest consisting of Japanese beech at the Appi tower site



Fig. 8.2 Warm temperate deciduous and evergreen mixed forest, predominantly consisting of Konara oak, at the Yamashiro tower site

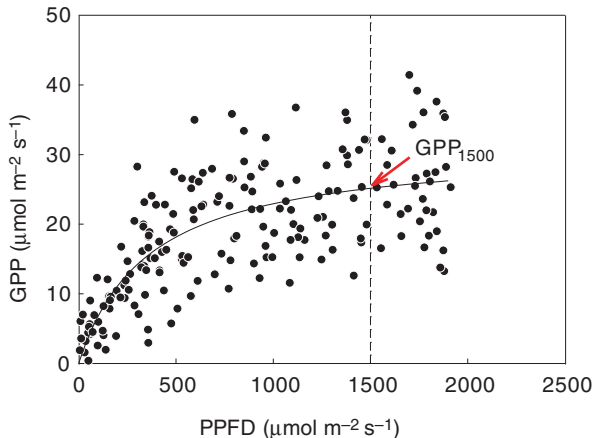


regenerated. The tree biomass (diameter at breast height [DBH] ≥ 3 cm) was estimated at 51 Mg C ha^{-1} in 1999, dominated by Konara oak, classified as a deciduous broadleaf tree species (66% of biomass), and *Ilex pedunculosa* Miq. (an evergreen broadleaf tree species; 28% of biomass) (Goto et al. 2003). The canopy height ranged from 6 to 20 m with an average of 12 m. The annual mean temperature was $14.7 \text{ }^{\circ}\text{C}$ (in 2000–2002), annual precipitation was 1,095 mm (in 2000–2002), and annual mean solar radiation was $11.9 \text{ MJ m}^{-2} \text{ day}^{-1}$ (in 2000–2002).

8.3 Estimation of Light-Saturated GPP

Light-saturated GPP was derived from the relationship between GPP and photosynthetic photon flux density (PPFD). The data were rejected when the friction velocity (u^*) was below 0.25 m s^{-1} , but in cases of precipitation, the data were included. We regressed the relation between GPP and PPFD as follows:

Fig. 8.3 Gross primary production (GPP) as a function of photosynthetic photon flux density (PPFD) in the beech forest, based on the pooled data of 9–10 weeks after the budbreak. Light-saturated GPP was determined as GPP at PPFD of 1,500 $\mu\text{mol m}^{-2} \text{s}^{-1}$



$$\text{GPP} = \alpha \text{GPP}_{\text{max}} \text{PPFD} / (\text{GPP}_{\text{max}} + \alpha \text{PPFD}) \tag{8.3}$$

where α denotes the ecosystem quantum yield and GPP_{max} the maximum GPP. We derived α and GPP_{max} for the pooled data at 2-week intervals from the onset of budbreak. We set the GPP at a PPFD of 1,500 $\mu\text{mol m}^{-2} \text{s}^{-1}$ based on the equation as the light-saturated GPP (Fig. 8.3).

The maximum light-saturated GPP of the beech forest varied among the years, but the environmental factors determining the inter-annual variation have not yet been fully identified (Yasuda et al. 2012). A survey of each individual tree suggested that the oak forest was still growing, as the total biomass increased from 2004 to 2009 (Kominami et al. 2012). Therefore, to investigate the O₃ effects on the seasonal changes in foliar photosynthetic maturation and senescence, we used a relative unit of GPP (GPP_{rel}), which is calculated as:

$$\text{GPP}_{\text{rel}} = \left(\text{light-saturated GPP} \right) / \left(\text{the maximum light-saturated GPP during the growth period for each year} \right)$$

The light-saturated GPP was estimated as the GPP at PPFD of 1,500 $\mu\text{mol m}^{-2} \text{s}^{-1}$ based on the GPP light-response curves derived from the pooled data for 2-week intervals from the budbreak. We categorized the growth season as spring–summer (April or May to July) for leaf maturation and summer–autumn (August to October or November) for leaf senescence stages.

8.4 Estimation of Cumulative O₃ Uptake (COU)

The approach used to estimate stomatal O₃ fluxes involves several steps, according to Cieslik (2004) and Gerosa et al. (2003). The aerodynamic resistance (R_a) is calculated from measured micrometeorological parameters such as friction velocity and sensible

heat flux by using the Monin–Obukhov similarity theory (see Gerosa et al. 2003, for calculation details), while the quasi-laminar layer resistance (R_b) is calculated by using the parameterization proposed by Hicks et al. (1987). We calculated the surface resistance (R_c) from the stomatal (R_{ST}) and non-stomatal resistance to O_3 (R_{NS}) as follows:

$$R_c = 1 / (1 / R_{ST} + 1 / R_{NS}) \quad (8.4)$$

$$R_{NS} = 1 / \left(\text{LAI} / r_{\text{ext}} + 1 / (R_{\text{inc}} + R_{\text{gs}}) \right) \quad (8.5)$$

where LAI is the leaf area index ($\text{m}^2 \text{m}^{-2}$), r_{ext} denotes the external leaf resistance, R_{inc} the in-canopy resistance, and R_{gs} the ground surface resistance. The maximum LAI in the beech forest was estimated from the amounts of leaf litter (Yasuda et al. 2012). Based on the field observations, we assumed that the LAI of the beech forest increased from 0 to the maximum within 1 month from the budbreak, and then decreased from the maximum to 0, also within 1 month, before the end of the foliage period. In contrast, seasonal changes in the LAI in the oak forest were measured using a plant canopy analyzer (LAI-2000; Li-Cor, Lincoln, NE, USA). The external leaf resistance (r_{ext}) is set at $2,500 \text{ s m}^{-1}$, the in-canopy resistance (R_{inc}) is defined as $b \text{ LAI} / h / u^*$, where h is the canopy height and b an empirical constant taken as 14 m^{-1} , and R_{gs} is set at 200 s m^{-1} (Erisman et al. 1994; Simpson et al. 2012).

The stomatal O_3 flux (F_{ST}) is obtained as follows:

$$F_{ST} = C_m * R_c / \left[(R_a + R_b + R_c) R_{ST} \right] \quad (8.6)$$

where C_m denotes the ozone concentration at the measurement height. The stomatal resistance (R_{ST}) is calculated by multiplying the stomatal resistance for water vapor flux (noted as R_s) by 1.65 (Gerosa et al. 2003). R_s is expressed as $1/G_s$, where G_s is determined from the modified BWB model described above (Eq. 8.2). We estimated C_m at the flux sites using the O_3 concentration data monitored by the nearest air pollution stations (Komatsu et al. 2015).

The COU in the forest ecosystem was calculated by summing up the ozone stomatal flux (F_{ST}) during the daytime (PPFD > 0) from the budbreak to a given period as follows:

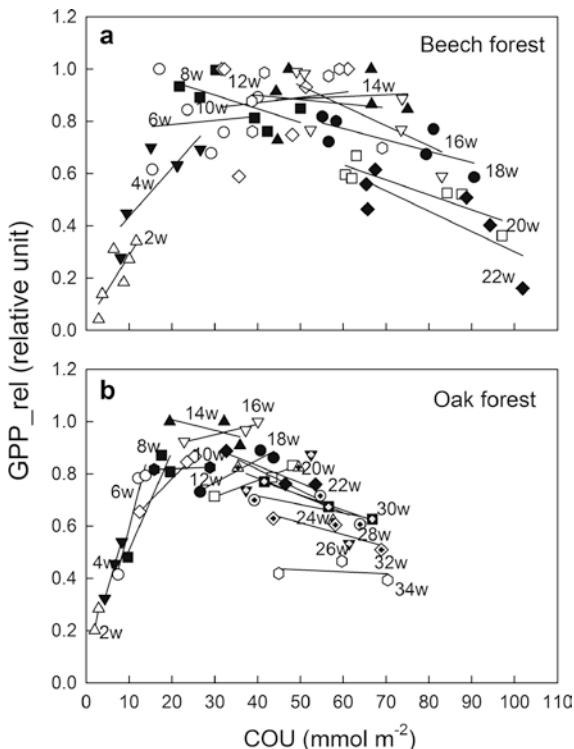
$$\text{COU} = \sum F_{ST} \Delta t, \quad (8.7)$$

where the mean daily sum of F_{ST} for the days of each month when F_{ST} data were available was substituted for the rest days when F_{ST} data were unavailable.

8.5 Effects of Cumulative O_3 Uptake (COU) on C Sequestering Capacity in the Beech and Oak Forests

To quantitatively evaluate the influence of the major explanatory factor(s) on the photosynthetic capacity, multiple regression analysis was used. We initially set four explanatory factors affecting potential photosynthetic performance

Fig. 8.4 Relationship between the relative unit of light-saturated GPP (shown as relative unit) and cumulative O₃ uptake (COU) at the end of each period from the budbreak in the beech (a) and oak (b) forests. Data are grouped by 2-week intervals from the budbreak, indicated by different symbols. Budbreaks in the beech forest occurred during April 30 to May 16, while those in the oak forest occurred during March 30 to April 8 (after Kitao et al. 2016)



(GPP_{rel}): leaf age, photoperiod, air temperature, and COU (Bauerle et al. 2012). GPP_{rel} in the spring–summer period could be explained by three explanatory factors, i.e., leaf age, photoperiod, and COU, in both the beech and oak forests. Increased COU, in addition to the photoperiod and leaf age, showed a positive effect on leaf maturation (Fig. 8.4a, b). As young leaves generally have less sensitivity to O₃ than old leaves (Kitao et al. 2015; Bohler et al. 2010), a stimulating effect of O₃ on photosynthesis at the early stage of leaf development needs to be further investigated. In contrast, GPP_{rel} in the summer–autumn period in the beech forest could be explained by two environmental factors, i.e., leaf age and COU. Thus, increased COU may accelerate age-dependent leaf senescence in the O₃-sensitive beech forest (Fig. 8.4a), whereas leaf senescence was not influenced by COU but was primarily influenced by air temperature in the O₃-tolerant oak forest (Fig. 8.4b). The lower O₃ sensitivity during leaf senescence in the oak forest may be attributed to the lower COU (due to the lower G_s) than in the beech forest (data not shown), as reported for the seedlings of Konara oak grown under free-air O₃ fumigation (Kitao et al. 2015).

8.6 Conclusion

In summary, our findings, based on long-term CO₂ flux observations, indicate that the photosynthetic C sequestering capacity of the forest ecosystem in an O₃-sensitive forest is potentially affected by the present-level O₃. O₃-induced earlier leaf senescence has been reported in several previous studies using open-top chambers and free-air fumigation systems (Karnosky et al. 2005; Kitao et al. 2009; Yamaji et al. 2003; Calatayud et al. 2011). In the present study, it is noteworthy that such accelerated leaf senescence induced by O₃ was apparently detected in the O₃-sensitive beech species at the real-world forest level. As the atmospheric O₃ concentrations are predicted to increase, particularly in East Asia, including Japan (Akimoto 2003; Karnosky et al. 2005; Ashmore 2005; Koike et al. 2013), earlier leaf senescence induced by elevated O₃ could cause further adverse effects on forest C sequestering in the future, particularly in forests consisting of O₃-sensitive species.

Acknowledgments Japan's Ministry of the Environment financially supported this study under a program of the Environment Research and Technology Development Fund (5B-1105, 2011–2013). We greatly appreciate Iwate prefecture and Kyoto prefecture for providing ground-based ozone data.

References

- Akimoto H (2003) Global air quality and pollution. *Science* 302:1716–1719
- Ashmore MR (2005) Assessing the future global impacts of ozone on vegetation. *Plant Cell Environ* 28:949–964
- Ball JT et al (1987) A model predicting stomatal conductance and its contribution to the control of photosynthesis under different environmental conditions. In: Biggens J (ed) *Progress in photosynthesis research*. Martinus-Nijhoff Publishers, Dordrecht, pp 221–224
- Bauerle WL et al (2012) Photoperiodic regulation of the seasonal pattern of photosynthetic capacity and the implications for carbon cycling. *PNAS* 109:8612–8617
- Biftu GF, Gan TY (2000) Assessment of evapotranspiration models applied to a watershed of Canadian Prairies with mixed land-uses. *Hydrol Proc* 14:1305–1325
- Bohler S et al (2010) Differential impact of chronic ozone exposure on expanding and fully expanded poplar leaves. *Tree Physiol* 30:1415–1432
- Calatayud V et al (2011) Responses of evergreen and deciduous *Quercus* species to enhanced ozone levels. *Environ Pollut* 159:55–63
- Cieslik SA (2004) Ozone uptake by various surface types: a comparison between dose and exposure. *Atmos Environ* 38:2409–2420
- Emberson LD et al (2000) Modelling stomatal ozone flux across Europe. *Environ Pollut* 109:403–413
- Erismann JW et al (1994) Parametrization of surface resistance for the quantification of atmospheric deposition of acidifying pollutants and ozone. *Atmos Environ* 28:2595–2607
- Fares S et al (2013) Testing of models of stomatal ozone fluxes with field measurements in a mixed Mediterranean forest. *Atmos Environ* 67:242–251
- Gerosa et al (2003) Micrometeorological determination of time-integrated stomatal ozone fluxes over wheat: a case study in Northern Italy. *Atmos Environ* 37:777–788
- Gerosa G et al (2005) Ozone uptake by an evergreen Mediterranean Forest (*Quercus ilex*) in Italy. Part I: micrometeorological flux measurements and flux partitioning. *Atmos Environ* 39:3255–3266

- Goto Y et al (2003) Aboveground biomass and net primary production of a broad-leaved secondary forest in the southern part of Kyoto prefecture, central Japan. *Bull FFPRI* 387:115–147 (in Japanese with English summary)
- Hicks BB et al (1987) A preliminary multiple resistance routine for deriving dry deposition velocities from measured quantities. *Water Air Soil Pollut* 36:311–330
- Karnosky DF et al (2005) Scaling ozone responses of forest trees to the ecosystem level in a changing climate. *Plant Cell Environ* 28:965–981
- Kitao M et al (2009) Effects of chronic elevated ozone exposure on gas exchange responses of adult beech trees (*Fagus sylvatica*) as related to the within-canopy light gradient. *Environ Pollut* 157:537–544
- Kitao M et al (2014) Seasonal ozone uptake by a warm-temperate mixed deciduous and evergreen broadleaf forest in western Japan estimated by the Penman-Monteith approach combined with a photosynthesis-dependent stomatal model. *Environ Pollut* 184:457–463
- Kitao M et al (2015) Growth over-compensation against O₃ exposure in two Japanese oak species, *Quercus mongolica* var. *crispula* and *Quercus serrata*, grown under elevated CO₂. *Environ Pollut* 206:133–141
- Kitao et al (2016) Increased phytotoxic O₃ dose accelerates autumn senescence in an O₃-sensitive beech forest even under the present-level O₃. *Sci Rep* 6:32549
- Koike T et al (2013) Effects of ozone on forest ecosystems in East and Southeast Asia. *Elsevier Dev Environ Sci* 13:371–390
- Komatsu M et al (2015) Estimation of ozone concentrations above forests using atmospheric observations at urban air pollution monitoring stations. *J Agric Meteorol* 71:202–210
- Kominami Y et al (2012) Heterotrophic respiration causes seasonal hysteresis in soil respiration in a warm-temperate forest. *J For Res* 17:296–304
- Matyssek R et al (2007) Promoting the O₃ flux concept for European forest trees. *Environ Pollut* 146:587–607
- Matyssek R et al (2010) Advances in understanding ozone impact on forest trees: message from novel phytotron and free-air fumigation studies. *Environ Pollut* 158:1990–2006
- Monteith JL (1981) Evaporation and surface temperature. *Q J R Meteorol Soc* 107:1–27
- Nagashima T et al (2003) The relative importance of various source regions on East Asian surface ozone. *Atmos Chem Phys* 10:11305–11322
- Ohara T et al (2008) Long-Term simulations of surface ozone in East Asia during 1980–2020 with CMAQ. In: Borrego C, Miranda AI (eds) *NATO science for peace and security series – C: environmental security, air pollution modelling and its application XIX*. Springer, Dordrecht, pp 136–144
- Richter A et al (2005) Increase in tropospheric nitrogen dioxide over China observed from space. *Nature* 437:129–132
- Simpson D et al (2012) The EMEP MSC-W chemical transport model – technical description. *Atmos Chem Phys* 12:7825–7865
- Yamaguchi M et al (2011) Experimental studies on the effects of ozone on growth and photosynthetic activity of Japanese forest tree species. *Asian J Atmos Environ* 5:65–78
- Yamaji K et al (2003) Ozone exposure over two growing seasons alters root-to-shoot ratio and chemical composition of birch (*Betula pendula* Roth). *Glob Chang Biol* 9:1363–1377
- Yasuda Y et al (2012) Carbon balance in a cool-temperate deciduous forest in northern Japan: seasonal and interannual variations, and environmental controls of its annual balance. *J For Res* 17:253–267